Choukri Bensalah[1], Amal Choukchou Braham [1], Rida Mokhtari [2]

Laboratoire d'automatique de Tlemcen (1),
École supérieure des sciences appliquées de Tlemcen (2),
University of Tlemcen, Algeria (1,2)

Modeling and Control of a Combined Inverted Pendulum on Beam System

Abstract. This paper addresses a novel structure for an underactuated system. It involves the combination of two well-known underactuated systems: the inverted pendulum-cart and the ball and beam. In this configuration, the cart in the first system replaces the role of the ball in the second. The primary focus lies in controlling the balancing beam, which is the key element of the system. The complete system is modeled using Lagrangian formulation, resulting in a set of coupled and highly nonlinear dynamical equations. Additionally, structural analysis of the corresponding control flow diagram is discussed. To control the entire system, an LQR controller with a PI controller in a cascade structure is employed. Simulation results demonstrate the stabilization performance of the proposed controller and its capability to address tracking problems.

Streszczenie. W artykule tym omówiono nową strukturę niedostatecznie aktywowanego układu. Obejmuje ona połączenie dwóch dobrze znanych niedostatecznie aktywowanych układów: odwróconego wózka wahadłowego oraz kuli i belki. W tej konfiguracji wózek w pierwszym układzie zastępuje rolę kuli w drugim. Główny nacisk położony jest na sterowanie belką równoważącą, która jest kluczowym elementem układu. Cały układ jest modelowany przy użyciu formuły Lagrange'a, co skutkuje zestawem sprzężonych i wysoce nieliniowych równań dynamicznych. Ponadto omówiono analizę strukturalną odpowiadającego schematu przepływu sterowania. Aby sterować całym układem, zastosowano regulator LQR z regulatorem PI w strukturze kaskadowej. Wyniki symulacji pokazują wydajność stabilizacji proponowanego regulatora i jego zdolność do rozwiązywania problemów ze śledzeniem. (Modelowanie i sterowanie kombinowanym odwróconym wahadłem na układzie belki)()

Keywords: Underactuated system, inverted pendulum, ball and beam, modelling, control flow diagram, LQR controller.
Słowa kluczowe: Układ niedostatecznie sterowany, wahadło odwrócone, kula i belka, modelowanie, schemat przepływu sterowania. \

Introduction

In practical control problems involving mechanical systems, fully actuated systems have the number of variables to be controlled equal to the input control number. However, in contrast, when the dimension of the configuration space exceeds that of the control input space, the system is termed underactuated or super-articulated. Such systems are increasingly vital in various domains, notably in space exploration. For instance, spacecraft launches can be likened to inverted pendulum-cart platform problems, while robots landing on planets often necessitate fewer actuators to minimize weight and energy consumption, often achieved through coupled joints [1]. These systems serve as fundamental frameworks for underactuated systems. Notable examples of underactuated mechanical systems include the rotating inverted pendulum, ball and beam, mass sliding on a cart, Acrobot, and Pendubot. Despite their seemingly simple structures, they provide valuable insights into controlling high-order underactuated real systems. Their common factor is the underactuation degree, which equals one and can be seen as unstable single-input multi-output (SIMO) systems. Recently, a novel and more complicated system has been proposed with one underactuation degree, where an inverted pendulum is mounted on a cart moving along a rail on a beam. This new mechanism is termed as the Inverted Pendulum Balancing on a Seesaw (IPBS) [2]. In addition to the cart carrying the pendulum, a second cart is affixed to the seesaw, moving parallel to the pendulum cart, allowing the seesaw to sway and maintain equilibrium. The resulting system has two inputs: the force applied to the pendulum cart to simultaneously control the cart's position and the pendulum's verticality, and the force applied to the second cart to maintain equilibrium. In summary, IPBS possesses two inputs and three outputs, constituting an unstable multi-input multi-output (MIMO) system. Similarly, within the same discipline, there exist other systems with more than one underactuation degree, including mobile robots, biped robots, swimming robots, quadrotors, and satellites. Unlike fully-actuated systems, underactuated systems are constrained in their control capabilities due to nonholonomic properties arising from non-integrable differential constraints. A comprehensive examination of both holonomic and nonholonomic properties is provided in [3], where eleven underactuated mechanical systems are discussed. Consequently, determining the controllability property, typically straightforward for fully-actuated systems, becomes locally challenging in underactuated systems. As a result, control synthesis for underactuated structures is inherently more complex. Seto and Baillieul, in [4], address control problems by categorizing underactuated systems into three structures: chain, tree, and isolated point, based on their Control Flow Diagram (CFD). This classification aids in predicting the feasibility of various control tools, such as feedback linearization and backstepping approaches. Furthermore, additional properties of underactuated systems, including relative degree, passivity, controllability, and control strategies, are discussed in [5, 6]. When it comes to control strategies, several approaches have been employed, broadly categorized into two parts: direct applications, mainly based on nonlinear methodologies, and indirect methods involving transformations of the system's state representation.

In direct approaches, nonlinear techniques such as robust nonlinear control [7, 8, 9], sliding mode control [10, 11, 12], energy-based control [13], fuzzy logic control [14], and optimal control [15] are commonly utilized.

Conversely, indirect methods involve altering the system's state representation through global or semi-global coordinate transformations, facilitating easier control application. This transformation can lead to the explicit representation of control for high-order underactuated systems in the form of a new cascade nonlinear system [16, 17].

Another approach involves input/output feedback linearization [19, 18], methods of approximate linearization pioneered by Hauser [20], saturation for stabilizing cascaded systems through feedforward, as proposed by Teel [21], and stabilization via output feedback, as developed by Teel and Praly [22]. In this paper, we propose a novel and more intricate dynamical structure surpassing the complexity of the IPBS. The mechanism involves integrating elements from both the inverted pendulum-cart platform and the ball and beam system, but without a counterweight. Specifically, the inverted pendulum typically carried by the cart is substituted for the ball and is allowed to roll along the beam. The primary
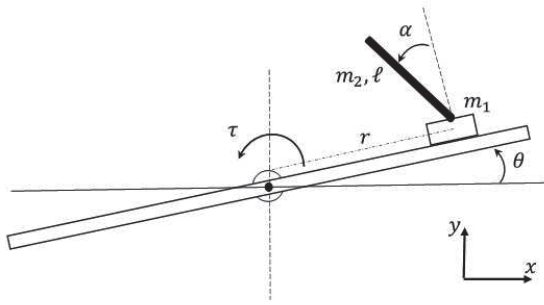
Fig. 1. Inverted pendulum on beam model

control objective is to maneuver the cart from any initial position to a desired position while simultaneously maintaining the verticality of the inverted pendulum and the horizontality of the beam. As a result, the resulting system exhibits two degrees of underactuation, as the only input available is the actuator mounted on the joint around which the beam pivots, with the cart rolling freely along the beam. Structurally, our proposed system bears resemblance to the IPBS. However, compared to the IPBS, our system exhibits greater complexity, as it requires managing two underactuation degrees. In the IPBS, only two inputs are utilized to control three states, resulting in a single degree of underactuation. In contrast, our system operates with a slower cart motion relative to the IPBS, as it is not directly propelled but instead influenced by gravity and beam inclination.

The stabilization objective of our system is significantly impacted by the cart weight and beam actuator acceleration. These factors have been carefully selected to align with our desired goals. Regarding the control approach, we advocate designing a Linear Quadratic Regulator (LQR) based on a linearized model. Furthermore, we propose implementing a PI controller in a cascade structure with the LQR to address tracking tasks. The paper also delves into the limitations of this controller concerning state variations and tackles the challenge of unavailable state measurements inherent in real-world experiments. This paper is organized as follows: In Section 2, we provide a detailed description of the proposed setup. Section 3 outlines the complete dynamical equations derived using the Lagrangian formulation. Following this, in Section 4, we discuss the structural properties of the proposed system, while Section 5 presents the control flow diagram. Subsequently, Sections 6 and 7 focus on the controller design and simulation results, respectively, aiming to provide comprehensive insights into the effectiveness of the proposed approach.

Setup description

The proposed Inverted Pendulum on Beam system (IPB) comprises a beam rotating around its fixed center. Along the beam, a cart moves and supports an inverted pendulum. The objective of this experiment is to keep the pendulum in its vertical position for any desired cart position. The schematic representation of the system, along with adopted coordinates and corresponding parameters, is depicted in Fig.1, where:
m_1 : Mass of the cart.
m_2 : Mass of the pendulum.
ℓ : Length of the pendulum.

$2L$: Length of the beam.
J : Inertia of the beam.
θ : Rotation angle of the beam.
α : Rotation angle of the pendulum.
r : Position of the cart.
τ : Input torque applied to the beam.
Here, the dynamical model of the actuator is not considered, simplifying the system input to be directly the torque applied. It is assumed that the cart position and the angles of both the beam and the pendulum are available.

System Modelling

Based on the principle of total energy conservation and utilizing the Lagrangian approach, we derive the equations describing the dynamics of the entire system. The Lagrangian equation is determined by considering the kinetic energy K and the potential energy P:

(1) $$L = K - P$$

where K and P are calculated as a sum of kinetic and potential energies of each system part, that is:

(2) $$K = K_{beam} + K_{cart} + K_{pendulum}$$
(3) $$P = P_{beam} + P_{cart} + P_{pendulum}$$

The beam

The kinetic energy of the beam is given by:

(4) $$K_{beam} = \frac{1}{2}J\dot{\theta}^2$$

Since the beam mass is assumed to be small, its potential energy is chosen to be zero.

The cart

The kinetic energy of the cart can be formulated as :

(5) $$K_{cart} = \frac{1}{2}m_1(\dot{r}^2 + r^2\dot{\theta}^2)$$

and the potential energy can be given as:

(6) $$P_{cart} = m_1 g r \sin(\theta)$$

The pendulum

Unlike the beam and the cart, the dynamical equation of the pendulum is too complicated since it depends on the dynamic of both above components. Here, it is assumed that the pendulum mass is located at the extremity as shows in Fig.1. Its kinetic energy can be expressed as:

$$K_{pendulum} = \frac{1}{2}m_2[\dot{r}^2 + r^2\dot{\theta}^2 + \ell^2(\dot{\theta} + \dot{\alpha})^2 - 2\ell(\dot{\theta} + \dot{\alpha})$$
$$\cdot [(\dot{r}\cos(\theta) - r\sin(\theta)\dot{\theta}) \cdot \cos(\theta + \alpha)$$
(7) $$+ (\dot{r}\sin(\theta) + r\cos(\theta)\dot{\theta}) \cdot \sin(\theta + \alpha)]]$$

and its corresponding potential energy is formulated as follows:

(8) $$P_{pendulum} = m_2.g.(r.\sin(\theta) + \ell.\cos(\theta + \alpha))$$

Leveraging the powerful symbolic computation toolbox of Matlab, we compute the three equations of motion for our

system using the general Lagrangian formulation:

(9)
$$\frac{\partial}{\partial t}\frac{\partial L}{\partial \dot{r}} - \frac{\partial L}{\partial r} = 0$$
$$\frac{\partial}{\partial t}\frac{\partial L}{\partial \dot{\theta}} - \frac{\partial L}{\partial \theta} = \tau$$
$$\frac{\partial}{\partial t}\frac{\partial L}{\partial \dot{\alpha}} - \frac{\partial L}{\partial \alpha} = 0$$

Once the above equations are symbolically computed, it is

possible to reformulate these equations in matrix form by adopting the following change $x = [x_1, x_2, x_3] = [r, \theta, \alpha]$ and $u = \tau$:

(10)
$$M(x)\ddot{x} + C(x,\dot{x}) + G(x) = F(x)u$$

where $M(x)$ is the inertial matrix, $C(x,\dot{x})$, $G(x)$ and $F(x)$ are Coriolis and centrifugal, gravitational and the input vectors, respectively, given by:

(11)
$$M(x) = \begin{bmatrix} m_1 + m_2 & -m_2\ell Cx_3 & -m_2\ell Cx_3 \\ -m_2\ell Cx_3 & J + \ell^2 m_2 + (m_1 + m_2)x_1^2 - 2m_2\ell x_1 Sx_3 & m_2\ell.(\ell - x_1 Sx_3) \\ -m_2\ell Cx_3 & m_2\ell.(\ell - x_1 Sx_3) & m_2.\ell^2 \end{bmatrix}$$

$$C(x,\dot{x}) = [-(m_1 + m_2)x_1\dot{x}_2^2 + m_2\ell Sx_3(\dot{x}_2^2 + \dot{x}_3^2 + 2\dot{x}_2\dot{x}_3);$$
$$- \ell m_2 x_1 Cx_3\dot{x}_3^2 - 2\ell m_2 x_1 \dot{x}_2 Cx_3\dot{x}_3 + 2m_1 x_1\dot{x}_1\dot{x}_2$$
$$- 2\ell m_2\dot{x}_1\dot{x}_2 Sx_3);$$

(12)
$$- \ell m_2(-x_1 Cx_3\dot{x}_2^2 + 2\dot{x}_1 Sx_3\dot{x}_2]$$

(13)
$$G(x) = \begin{bmatrix} (m_1 + m_2)gSx_2 \\ -\ell gm_2 S(x_2 + x_3) + m_1 gx_1 Cx_2 + gm_2 x_1 Cx_2 \\ gS(x_2 + x_3)) \end{bmatrix}$$

and

(14)
$$F(x) = \begin{bmatrix} 0; 1; 0 \end{bmatrix}^T$$

It can be shown that the inertial matrix is a symmetric and positive defined matrix, its determinant is given by:

(15)
$$det(M) = \ell^2 m_2(m_1 x_1^2(m_1 + m_2) + Jm_1 + Jm_2 S(x_3)^2)$$

Then, we conclude that $\forall x \in \mathbb{R}^3$, $det(M) > 0$. Thus, M is an invertible matrix allowing to rewrite Eq.10 as :

(16)
$$\ddot{x} = H(x,\dot{x},u)$$

This form will be used in the control flow diagram analysis. Moreover, Eq.10 can also be expressed in the nonlinear control affine system form:

(17)
$$\dot{x} = f(x) + g(x)u$$

Structural properties of the IPB system
Local behaviour

Equilibrium points of the system described by Eq.17 are given by resolving the system:

(18)
$$\dot{x} = 0$$

Solving this last equation by MATLAB yields to 19 solutions where only two solutions are physicly realisable; $x_{eq_1} = [0, 0, 0]$ and $x_{eq_2} = [0, 0, \pi]$. Here, we are interested by the first configuration. The second one can be used for swing-up task [**?**]. Furthermore, near equilibrium, the control input vanishes and does not appear in the system equations. The

Jacobian matrix at x_{eq_1} is given by:

(19)
$$A = \frac{1}{d}\begin{bmatrix} 0 & 0 & 0 & 1 & 0 & 0 \\ 0 & 0 & 0 & 0 & 1 & 0 \\ 0 & 0 & 0 & 0 & 0 & 1 \\ 0 & -g & \frac{gm_2}{m_1} & 0 & 0 & 0 \\ -\frac{g(m_1+m_2)}{J} & 0 & 0 & 0 & 0 & 0 \\ \frac{g(m_1+m_2)}{J} & 0 & \frac{g(m_1+m_2)}{\ell m_1} & 0 & 0 & 0 \end{bmatrix}$$

where $d = \frac{g^3(m_1+m_2)^2}{J\ell m_1}$.
The control vector B is given by:

(20)
$$B = \frac{1}{d}\begin{bmatrix} 0 \\ 1 \\ -1 \end{bmatrix}$$

The linearized system is controllable and can be written as:

(21)
$$\dot{x} = Ax + Bu$$

while the observer equation is given by:

(22)
$$y = Cx + Du$$

with :

(23)
$$C = \begin{bmatrix} 1 & 0 & 0 & 0 & 0 & 0 \\ 0 & 1 & 0 & 0 & 0 & 0 \\ 0 & 0 & 1 & 0 & 0 & 0 \end{bmatrix} \text{ and } D = \begin{bmatrix} 0 \\ 0 \\ 0 \end{bmatrix}$$

The parameters of the preceding equations are defined as follows: $m_1 = 0.8\ kg$, $m_2 = 0.065\ kg$; $J = 1\ kg\ m^2$ and $\ell = 0.5\ m$. These parameters are chosen to be as similar as possible to the inverted pendulum and the ball and beam systems of Quanser didactic experimental setups [23]. Computing the eigenvalues of A reveals two real eigenvalues in the right half plane, two real eigenvalues in the left half plane, and two eigenvalues on the imaginary axis. Consequently, the proposed system is unstable and exhibits oscillatory behavior.

Control Flow Diagram
    Despite the controllability of the linearized system, devising a robust control strategy for the entire system is not a straightforward endeavor. In [5], the authors suggested potential control strategies based on a classification derived from an examination of the associated Control Flow Diagram (CFD) [19]. The CFD depicts the transmission of control

through degrees of freedom (DOF) and the interaction between them. Three distinct structures are identified: chain, tree, and isolated vertices.Fig.**??** (a), (b), (c) respectively.

The first structure is the least complex one to be controlled, where both, feedback linearization technique and backstepping strategy can be applied. In contrast, a system with a tree structure poses more challenges for control since one control input must act on multiple degrees of freedom simultaneously. Furthermore, for systems with an isolated vertices structure, achieving certain control objectives can be difficult or even impossible because the control does not influence some variables, particularly when the relative degree is not well-defined. Moreover, positive or negative values are assigned to links, indicating whether the interactions are strong or vanish, respectively, for certain values of the states.

For a system described by $\ddot{q} = H(q, \dot{q}, \tau)$ and an equilibrium point $(q^0, \dot{q}^0)$, theses values are given by:

$$
(24) \quad
\begin{cases}
2 & \text{if } \dfrac{\partial H_i}{\partial \tau_j} \neq 0 \text{ at } (q^0, \dot{q}^0) \\[2mm]
-2 & \text{if } \dfrac{\partial H_i}{\partial \tau_j} \neq 0 \ \forall (q, \dot{q}) \in U \text{ except at } (q^0, \dot{q}^0) \\[2mm]
1 & \text{if } \dfrac{\partial H_i}{\partial \dot{q}_k} \neq 0 \text{ at } (q^0, \dot{q}^0) \\[2mm]
-1 & \text{if } \dfrac{\partial H_i}{\partial \dot{q}_k} \neq 0 \ \forall (q, \dot{q}) \in U \text{ except at } (q^0, \dot{q}^0) \\[2mm]
2 & \text{if } \dfrac{\partial H_i}{\partial \dot{q}_k} \equiv 0 \ \forall (q, \dot{q}) \in U \ \text{and } \dfrac{\partial H_i}{\partial q_k} \neq 0 \text{ at } (q^0, \dot{q}^0) \\[2mm]
-2 & \text{if } \dfrac{\partial H_i}{\partial \dot{q}_k} \equiv 0 \ \forall (q, \dot{q}) \in U \text{ and } \dfrac{\partial H_i}{\partial q_k} \neq 0 \ \forall (q, \dot{q}) \in U \\[1mm]
& \text{except at } (q^0, \dot{q}^0)
\end{cases}
$$

From a controllability standpoint, a degree of freedom (DOF) is considered directly controllable when the length from the input to this DOF is 2. Conversely, it is indirectly controllable when this length exceeds 2. In both cases, the relative degree is well-defined. However, if the length from the input to the DOF is less than 2, the relative degree is not well-defined. Otherwise, the relative degree is not well defined.

To construct the CFD of the proposed system, let first define the CFD of each subsystem. In [5], it was shown that the inverted pendulum has a tree structure Fig.2.(a), whereas, the ball and beam system has an isolated vertex Fig.2.(b).
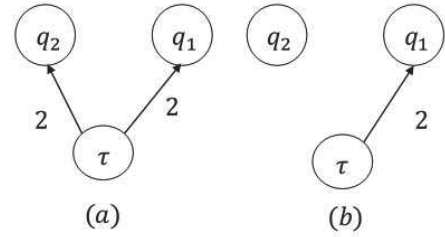

Fig. 2. CFD structures for inverted pendulum (a) and ball on beam systems (b).

For the IPB system, the associated CFD includes three vertices representing the three DOF and one vertex for the control. From Eq.16 and according to Eq.24, the following results allow to weigh links between each DOF and the input:

$$\frac{\partial H_1(\dot{x}, x, u)}{\partial x_4} = \frac{2Jm_2 x_5 sin(2x_3)}{det(M)}$$

$$\frac{\partial H_1(\dot{x}, x, u)}{\partial x_5} = \frac{2x_1 x_5(x_1 m_1 + J)(m_1 + m_2) - 2\ell m_2(x_1^2 + J) - 2\ell m_2 sin(x_3)(m_1 x_1^2 + J)(x_5 + x_6) + Jm_1 x_4 sin(2x_3) - 2JM x_1 x_5 cos(x_3)^2}{det(M)}$$

$$\frac{\partial H_1(\dot{x}, x, u)}{\partial x_6} = \frac{-2Lm_2 sin(x_3)(m_1 x_1^2 + J(x_5 + x_6))}{det(M)}$$

(25)

$$\frac{\partial H_1(\dot{x}, x, u)}{\partial u} = \frac{m_2 x_1 sin(2x_3)}{det(M)}$$

$$\frac{\partial H_2(\dot{x}, x, u)}{\partial x_4} = \frac{-2m_1 x_1 x_5(m_1 + m_2)}{det(M)}$$

$$\frac{\partial H_2(\dot{x}, x, u)}{\partial x_5} = \frac{-(2m_1 x_1((m_1 + m_2)x_4 - \ell m_2 cos(x3))(x_5 + x_6))}{det(M)}$$

$$\frac{\partial H_2(\dot{x}, x, u)}{\partial x_6} = \frac{2\ell m_1 m_2 x_1 cos(x_3)(x_5 + x_6)}{det(M)}$$

(26)

$$\frac{\partial H_2(\dot{x}, x, u)}{\partial u} = \frac{m_1 + m_2 - m_2 cos(x_3)^2}{det(M)}$$

$$\frac{\partial H_3(\dot{x}, x, u)}{\partial x_4} = \frac{2x_5(m_1 + m_2)(Jsin(x_3) + \ell m_1 x_1)}{det(M)}$$

$$\frac{\partial H_3(\dot{x}, x, u)}{\partial x_5} = \frac{2(Jx_4 sin(x_3) + \ell x_1 x_4 m_1)(m_1 + m_2) - (J\ell m_2 sin(2x_3) - 2\ell^2 m_1 m_2 x_1 cos(x_3))(x_5 + x_6)}{det(M)}$$

$$\frac{\partial H_3(\dot{x}, x, u)}{\partial x_6} = \frac{-(m_2(x_5 + x_6)(Jsin(2x_3) + 2\ell m_1 x_1 cos(x_3)))}{det(M)}$$

(27)

$$\frac{\partial H_3(\dot{x}, x, u)}{\partial u} = \frac{-(\ell m_1 - (m_1 + m_2)x_1 sin(x_3) + \ell m_2 sin(x_3)^2)}{det(M)}$$

Eq.25 shows that the right term can vanish for $x_1 = 0$ or $x_3 = 0$. Whereas, Eq.26 is never equal zero, as well as Eq.27. As a result, the link of u/x_1 is weighted with -2 and both u/x_2, u/x_3 take 2. The rest of different links are

weighted by -1. The resulting CFD is depicted in Fig.3(a) and the final one is obtained by eliminating all links with negative value Fig.3(b) . As expected results, the CFD for the whole system exhibits a tree-isolate point structure. This in-
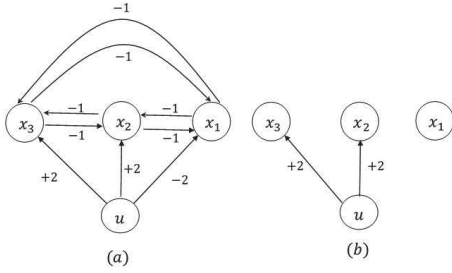
Fig. 3. Control Flow Diagram before (a) and after simplification

dicates that the nonlinear control design for such structu rather complicated. In the next section, a linear control sign for local stabilization problem is proposed. The obta results are then extended to cover the cart position trac task.

Controller design

Based on the IPB linearized state-space model, the I is adopted to solve the control problem. The cost func $J = \int_0^\infty (x^T Q x + u^T R u) dt$ is minimized to find a com mise between the energies of states $x^T Q x$ and system input $u^T R u$. The control law is in the form of $u = -Kx$ where $K = R^{-1} B^T P$ is the gain matrix and P is the solution of Ricatti equation $A^T P + P A - P B R^{-1} B^T P + Q = 0$. Matrices Q and R are positive-semi definite and positive definite, respectively. They play the role of weighting factors by allowing to give importance to one of the two energies.

Despite the stabilization of IPB around the equilibrium point, the LQR controller is not able to lead with tracking problem for $x_1 = r_d \neq 0$ owing to the accumulation of the output error. To overcome this problem, we use a PI controller where the output is injected into the LQR controller. Here, we adopt for PI parallel structure with gains $K_p = 1$ and $T_i = 0.3$. According to LQR controller and Matlab tool, the gain vector K is computed by choosing the following weighting matrices $Q = diag(5000, 1, 1, 0, 0, 0)$ and $R = 0.1$. This choice means that our interest focuses more on the cart position state variable than the rest. In addition, the control signal should be relatively small owing to the high sensitivity of the system. In the experimental case, another problem should be resolved related to measurements availability, knowing that the LQR controller imply all state variables in the control law, while only three states are measured at the output (Eq.23). In fact, the time derivative of the state variables ($\dot{r}, \dot{\alpha}, \dot{\theta}$) are explicitly derivated by using a time derivative action. However, this action can greatly amplify the noise and can not be really realised. In order to overcome this drawback, a dirty-derivative can be used. Each state variable is passed through a filter taking the following form : $H(s) = \frac{s}{\varepsilon s + 1}$ with $\varepsilon > 0$ being sufficiently small. However, when the outputs exhibit abrupt change, a large values of the signal derivatives could be arisen and can destabilize the closed loop system. A simple cure of this problem is to limit the control signal to be adequate by using a saturation block. The controller scheme of the IPB can be summarized by the Fig.4.

Simulation results

The proposed IPB system in closed loop structure using the LQR controller has been simulated and evaluated in two phases by means of library Simulink of Matlab. First, only the LQR controller is used to stabilize the system around the origin point $(0, 0, 0)$. Next, the LQR parameters are used
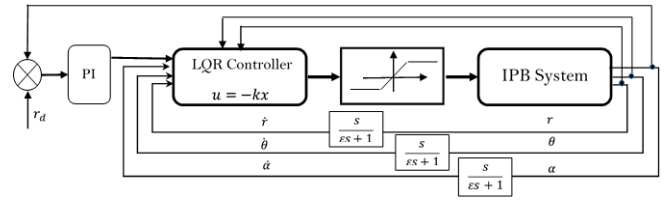

Fig. 4. Closed loop diagram with LQR controller and dirty-derivative estimator
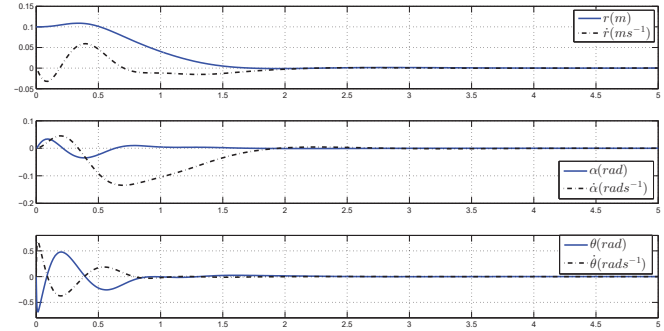

Fig. 5. State variables for stabilization problem using LQR controller

for tracking problem using a PI controller. By exploiting the previously defined weighting matrices Q and R, the resulting state feedback gain vector is :

$$K = (99.8; -857.2; -1318.0; 158.8; -303.7; -336.7)$$

To avoid peaking phenomenon of the control signal, the saturation function is defined as:

$$(28) \quad u = \begin{cases} u & if & |u| \leq 35 \, (Nm) \\ 35 & if & u > 35 \, (Nm) \\ -35 & if & u < -35 (Nm) \end{cases}$$

The simulation results of this first part are depicted in Fig.5 and Fig. 6. As can be shown in Fig.5, the angle error of the inverted pendulum has been firstly vanished and after that of the beam and the latest was the cart position. During many trials, it has been noted that the output signals are strongly dependant on the choice of initial conditions. For small initial condition value of α and owing to the high value of the feedback gain vector K, it can lead to physically unrealizable configurations ($\alpha > \frac{pi}{2}$).

In the second part, a PI controller is placed before the LQR controller to achieve tracking task for the cart position. Fig.7 and Fig.8 show the simulation results of PI with LQR controllers in cascade form for desired position $r_d = 0.5 \, m$. As expected from the previous simulation, the angle error for both inverted pendulum and beam vanished in short time, unlike the cart position allure which takes more time to reach the target. The signal control is stabilized around a non-zero value to ensure an adequate torque engendered by the non-zero desired cart position.

Conclusion

The main objective of this work is to develop and control a new underactuated mechanical system. It consists of the inverted pendulum installed on the cart rolling on rotated beam. The obtained linear model shows the unstability of the SIMO system. In order to describe more the system be-
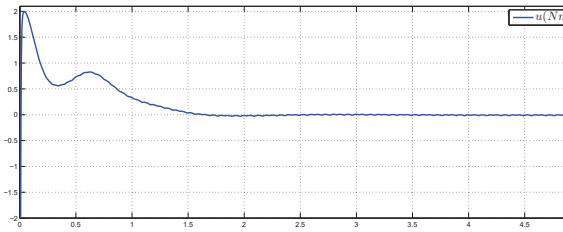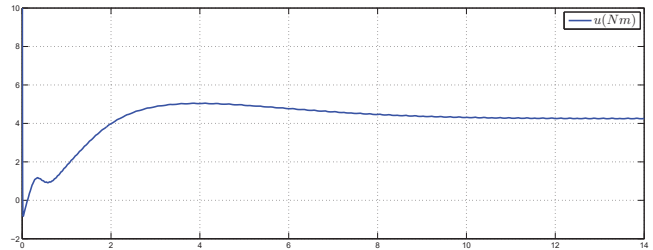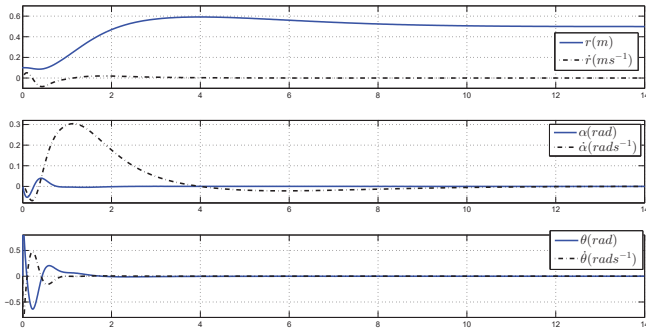
Fig. 6. Signal control

Fig. 7. State variables for tracking problem using PI and LQR controllers for $r_d = 0.5\ m$

Fig. 8. Signal control of PI and LQR controllers

haviour and to provide for an adequate controller, the associated CFD has been developed. After simplification, the CFD analysis shows the direct impact of the control on the beam rotation and the inverted pendulum inclination, unlike the cart position. This phenomenon is explicitly shown while the LQR controller evaluation. The PI controller is placed in cascade structure with the LQR to achieve a tracking task of the cart position. The simulation results showed the sensitivity of the inverted pendulum behaviour with respect to its initial value owing to the high value of gain vector of the closed loop. Our expected future work will focus on experimental realization of the IPB and apply the effect of dirty-derivative filter to estimate unavailable variables.

Authors: *Ph.D. Choukri Bensalah, Laboratoire d'automatique de Tlemcen (LAT), Department of Electrical and Electronics Engineering, Faculty of Technology, University Abou Bekr Belkaid, Chetouane B.P 230 Tlemcen, Algeria. email: choukribensalah@gmail.com, choukri.bensalah@univ-tlemcen.dz, Pr. Choukchou Braham Amal, Laboratoire d'automatique de Tlemcen (LAT), Department of Electrical and Electronics Engineering, Faculty of Technology, University Abou Bekr Belkaid, Chetouane B.P 230 Tlemcen, Algeria. email: amal.choukchou@gmail.com*

REFERENCES
[1] Bensalah C., Quijano J., Hendrich N., Abderrahim A. Anthropomorphic robotics hand inverse kinematics, 16th International Conference on Advanced, Robotics (ICAR) , 2013;.
[2] J Lin., Chang.: Stabilization and equilibrium control of a new pneumatic cart-seesaw system. Robotica, 26, pp.219–227,2008.
[3] Yu.: A survey of underactuated mechanical systems, IET Control Theory and Applications, 7, pp. 921–935, 2013.
[4] Baillieul.: Control problems in super-articulated mechanical systems, IEEE Trans Autom Control, 39, pp. 2442 – 2453, 2013.
[5] A. Choukchou-Braham.: Analysis and control of underactuated mechanical systems, Springer, 2014.
[6] Kokotovic.: Nonlinear control via approximate input-output linearization: The ball and beam example., IEEE Transactions on Automatic Control, 37, pp. 392–398, 1992.
[7] Jie Huang., Ching-Fang Lin.: Robust nonlinear control of the ball and beam system., Proceedings of 1995 American Control Conference - ACC'95, Seattle, WA, USA, 1, pp. 306-310, 1995.
[8] A T Simmons., J Y Hung.: Hybrid control of systems with poorly defined relative degree: the ball-on-beam example, 30th Annual Conference of IEEE Industrial Electronics Society, 2004. IECON 2004, Busan, Korea (South), 3, pp. 2436-2440, 2004.
[9] Y Fang, B Ma, P Wang., X Zhang.: A Motion Planning-Based Adaptive Control Method for an Underactuated Crane System, IEEE Transactions on Control Systems Technology, 20, pp. 241-248, Jan. 2012.
[10] A. Choukchou-Braham., C. Bensalah., B. Cherki.: Stabilization of an under-actuated mechanical system by sliding mode control, Proc 1st Conf on Intelligent Systems and Automation CISA, 1019, pp. 80–84, June 2008.
[11] Rong Xu., Ümit Özgüner.: Sliding mode control of a class of underactuated systems, Automatica, 1019, pp. 233-241, January 2008.
[12] Van, M., Chen, L.: Sliding Mode Control of a Class of Underactuated System With Nonintegrable Momentum, Journal of the Franklin Institute, 1019, pp. 9484-9504, 2020.
[13] Mark W. Spong.: Energy Based Control of a Class of Underactuated Mechanical Systems, 13th World Congress of IFAC, San Francisco USA, 29(1), pp. 2828-2832, 1996.
[14] Xiaorong Huang https., Anca L Ralescu anca., Haibo Huang.: A survey on the application of fuzzy systems for underactuated systems, Proceedings of the Institution of Mechanical Engineers, Part I: Journal of Systems and Control Engineering, 233(3), pp. 217-244, 2019.
[15] I Hussein., A M Bloch.: Optimal Control of Underactuated Nonholonomic Mechanical Systems, IEEE Transactions on Automatic Control, 53(3), pp. 668-682, April. 2008.
[16] Olfati-Saber, R.: Nonlinear control of underactuated mechanical systems with application to robotics and aerospace vehicles, PhD dissertation, Department of Electrical Engineering and Computer, Massachusetts Institute of Technology, 2001.
[17] Park, M.S., Chwa, D.K.: wing-up and stabilization control of inverted-pendulum systems via coupled sliding-mode control method, IEEE Trans. Ind. Electron, 56,pp. 3541–3555, 2009.
[18] Hauser, J., Sastry, S., Kokotovico, P.: control via approximate input-output linearization: the beam and ball example, IEEE Trans. Autom. Control, 37, pp. 392–398, 1992.
[19] Atal Anil Kumar., Jean-François Antoine., Gabriel Abba.: Optimal Input-Output Feedback Linearization for the Control of a 4 Cable-Driven Parallel Robot, IFAC-PapersOnLine, 52, pp. 707-712, 2019.
[20] J Hauser.: Nonlinear control via uniform nonlinear system approximation, IEEE Control and Decision Conference,. 1990.
[21] R Lozano., Bernard Brogliato., Ioan Doré Landau: Passivity and Global Stabilization of Cascaded Nonlinear Systems, IEEE Transactions on Automatic Control, 37(9), pp. 1386 - 1388, October. 1992.
[22] M W Spong., L Praly., Bernard Brogliato., Ioan Doré Landau: of underactuated mechanical systems using switching and saturation, Control Using Logic-based Switchin. Ed. A. S. Morse, Springer, 222, pp. 162-172.
[23] Mohammad Keshmiri., Ali Fellah Jahromi., Abolfazl Mohebbi., Mohammad Hadi Amoozgar., Wen-Fang Xi: Modeling and control of ball and beam system using model based and non-model based control approaches, Iternationam Journal on smart sensing and intelligent systems , 5(1), pp. . 14-35, March. 2012.